N-terminal modification of Histone H3 inhibits H3K27M-mediated loss of H3K27 trimethylation

Nicolas Poux[1-3], Daren F Zhang[2,3], Adam F Kebede[2,3], Isabella Gainey[2], Olohireme E Famous[2], Rameen Beroukhim[3-5], and Pratiti Bandopadhayay[2,3,6*]

Affiliations

1. Harvard/MIT MD-PhD Program, Harvard Medical School, Boston, MA, USA

2. Department of Pediatric Oncology, Dana-Farber Boston Children's Cancer and Blood Disorders Center, Boston, MA, USA

3. Broad Institute of MIT and Harvard, Cambridge, MA, USA

4. Departments of Cancer Biology and Medical Oncology, Dana-Farber Cancer Institute and Harvard Medical School, Boston, MA, USA

5. Department of Medicine, Harvard Medical School, Boston, MA, USA

6. Department of Pediatrics, Harvard Medical School, Boston, MA, USA

* Corresponding author

Abstract

The use of short epitope tags is widespread in the study of histone H3 biology as they allow for the antibody-mediated detection and pulldown of particular histone post-translational modifications (PTM) or exogenous histone transgenes. However, H3 is particularly sensitive to sequence modification and the addition of epitope tags may interfere with the native function of H3. Here, we use the known relationship between lysine-to-methionine K27M mutations and the loss of trimethylation at the H3 K27 residue to test whether the addition of epitope tags to the N or C terminus of H3 affects the levels of histone H3 PTMs. We find that all tested N-terminal tags abrogate the H3K27M-mediated loss of H3K27 trimethylation. These results suggest that the addition of epitope tags to the N-terminus of H3 should be performed with caution, and these findings may be of particular interest for the study of H3-driven cancers, like diffuse midline gliomas.

Introduction

Post-translational modification of the N-terminal tail of histone H3 is a central mechanism driving the formation of epigenetic states[1]. Mutations in this tail sequence alter the ability of histone modifiers and readers to bind to the tail, leading to epigenetic dysregulation and have been associated with developmental disorders and cancers. Lysine 27 is a key regulatory site and K-to-M mutations at this position (H3K27M) block the deposition of the repressive H3K27me3 mark and are the initiating genomic event in diffuse midline gliomas, a fatal pediatric brain tumor[2–4].

The sequence similarity of H3K27M to wild-type H3 renders the study of the mutation difficult without the use of epitope tags. These tags are short amino-acid sequences that provide a specific binding motif for antibody-mediated detection and pulldown of proteins. Epitope tags have been foundational in establishing the oncogenic role of H3K27M right from the earliest cellular models demonstrating that fractional expression of H3K27M induced the loss of H3K27me3[4], to more recent papers studying the mechanisms and extent of epigenetic reprogramming induced by H3K27M[5–7].

However, the heavily conserved histone proteins show an exquisite sensitivity to sequence alterations. Even the five amino acid differences between the H3 variants H3.1 and H3.3 are sufficient for them to be deposited into nucleosomes using separate molecular machinery[8–11]. As such, it is possible that the addition of epitope tags may interfere with the function of endogenous H3 or the H3K27M mutant.

There is little consensus on the best practices for the use of epitope tags in the DMG literature. The most commonly used tags, FLAG, HA, and V5, possess different features that might uniquely affect H3 function: FLAG is enriched for negative side chains, HA contains many bulky tyrosines and prolines, and V5 is nearly twice as large as the other two. Additionally, the location of the tag carries different implications: the H3 N-terminus contains the unstructured histone tail where post-translational modifications are deposited, whereas the C-terminus forms the histone core that determines the strength of H3-DNA binding interaction. Many seminal papers in the DMG field differ in the identity and location of the tag used, introducing a potential source of variability across findings[4,7,12–14].

We thus hypothesized that the addition of N-terminal epitope tags might disrupt essential functions of the histone H3 tail. In this study, using the established relationship between H3K27M expression and loss of H3K27me3 levels, we test whether epitope tags disrupt the effects of the H3K27M mutation when added to the N-terminal histone tail.

Results

Many DMG models harness lentivirus-mediated overexpression systems to introduce the mutant H3K27M into human neural stem cells (hNSC). We first sought to generate such models, leveraging lentiviral vectors to induce expression of H3.3, including both the wild-type and K27M mutant transcripts, without any tag. In iPSC-derived hNSCs, expression of untagged K27M mutant H3.3 (H3.3K27M) was sufficient to cause a significant reduction in H3K27me3 levels compared to untransduced cells or to the wild-type H3.3 (H3.3WT) controls (Figure 1). The level of suppression of H3K27me3 was of a similar magnitude to that observed in patient-derived H3.3K27M mutant DMG cell

line BT245. We conclude that the overexpression of H3.3K27M is sufficient to suppress the polycomb repressive mark H3K27me3, as previously reported[4,7,12].

We next evaluated whether similar suppression of H3K27me3 is observed with the introduction of N-terminal tags. We generated lentivirus overexpression constructs encoding either wild-type (WT) H3.1 or H3.3, or the K27M mutants (H3.1K27M and H3.3K27M). We then added a FLAG-HA tag, which was used in the original cellular models describing H3K27M-induced loss of H3K27me3, to the N-terminus of the H3 gene coding sequence. After transducing hNSCs with the lentivirus containing N-terminus tagged H3 constructs, or the untagged H3.3K27M, we compared H3K27me3 levels of our tagged and untagged hNSCs against patient derived H3.3K27M DMG lines (BT245, SF7761) using Western immunoblotting. We confirmed that overexpression of untagged H3.3K27M was sufficient to cause a significant reduction in H3K27me3 levels (20.7% of untransduced NSCs, p=0.0058), whereas untagged H3.3WT did not lead to a reduction in H3K27me3 (Figure 2). However, we observed no similar reduction in H3K27me3 levels in either the N-terminus FLAG-HA tagged H3.1K27M (118.3% of untransduced NSC) or H3.3K27M (117.5% of untransduced NSC), despite observing that H3.3K27M expression was comparable between the tagged hNSC, untagged hNSC, and the BT245 DMG line using an H3.3-specific anti-H3K27M antibody.

Prior work evaluating the cellular hierarchy of diffuse midline gliomas has highlighted that H3.1 and H3.3 K27M mutant gliomas likely have different cells of origin, arising from distinct waves of oligodendrocyte precursor cell (OPC) specification[15]. This raises the possibility that the histone mutations may exert their phenotypes in specific cellular contexts. We therefore evaluated whether the lack of suppression of H3K27me3 observed in the setting of N-terminal tags on the mutant histone varied across different cell types. We transduced human embryonic stem cell (hESC)-derived OPCs or HEK293T cells, human embryonic kidney cells that were used in the original demonstration of the effects of H3K27M on H3K27me3, to overexpress the same N-terminus tagged H3.1K27M or H3.3K27M constructs. Within these contexts, expression of N-terminus tagged H3.3K27M did not result

in a reduction of H3K27me3 levels (Figure 2), though expression of N-terminal tagged H3.1K27M in HEK293Ts was associated with a mild reduction in H3K27me3 (47.7%, p=0.0502).

To determine whether the tag peptide sequence itself interfered with the ability of H3K27M to suppress the H3K27me mark, we generated an additional panel of H3.3WT or K27M expressing NSCs, in which the K27M mutants were tagged with either V5, FLAG or HA. However, we did not observe any suppression of the H3K27me3 marks with expression of any of the N-terminal tags on H3.3 K27M (Figure 3), suggesting that the presence of any N-terminal H3.3 tag may interfere with downstream functions of the K27M mutation.

Finally, we evaluated whether C-terminal tags similarly interfered with the ability of H3K27M to suppress H3K27me3 in NSCs by adding a FLAG-HA tag to the C-terminus of H3.3K27M. In this context, NSCs transduced to express C-terminal FLAG-HA H3.3K27M exhibited a significant reduction in H3K27me3 levels (30.3% of untransduced NSCs, p=0.032, Figure 3) that was similar in magnitude to the effect seen with untagged H3.3K27M (34.5% of untransduced NSC, p=0.043). This suggests that the addition of tags to the N-terminus may be especially inhibitory to H3K27M function relative to C-terminal tagging.

Discussion

We have found that overexpression of N-terminus tagged histone H3 K27M attenuates its suppression of H3.3K27me3 across multiple contexts, including distinct protein tags. This presents the possibility that N-terminal tags disrupt H3 functions. This has significant implications for the design and generation of models to study H3.3 K27M mediated oncogenicity, particular in the context of Diffuse Midline Gliomas.

This study has several limitations. It does not establish whether N-terminal epitope tags prevent the loss of H3K27me3 by disrupting the incorporation of the exogenous tagged-H3 into nucleosomes, or whether it interferes with the binding of the PRC2 complex or other histone modifiers at the tail of the incorporated histone. Additionally, we do not establish whether the same process that disrupts the loss

of H3K27me3 in N-terminus tagged H3 would similarly affect PTMs at other sites on the H3 tail. Finally, our model systems rely on exogenous overexpression of the mutant histone which may be associated with additional artifacts. It will be important to assess the effects of N- and C-terminal tags on function of the K27M mutations in the endogenous setting.

Our results support the idea that epitope tags should be used with caution when studying histone biology, and that the N-terminal tail is an unideal location for the addition of such tags when modeling DMGs. Furthermore, in the context of H3K27M mutations, these findings may explain the heterogeneity that we have observed in the magnitude of H3K27me3 reductions resulting from H3K27M expression across published results using different H3 tags. Taken together, these findings emphasize the need for careful validation of histone function when using modified histones and may warrant further investigation to determine whether N-terminal tags disrupt other H3-tail PTMs beyond H3K27me3.

Materials and Methods

Cell line models

Cell line authentication and mycoplasma testing.

Human neural stem cells (hNSC) (ACS-5004) were purchased from American Type Culture Collection (Manassas, VA, USA). Lenti-X 293T cells were purchased from Takara Bio (Shiga, Japan). hESC-derived OPCs were purchased from EMD Millipore Sigma (SCR600). SF7761 patient-derived DMG cell line was purchased from Sigma Aldrich (SCC126). BT245 patient-derived DMG line (RRID:CVCL_IP13) was a gift from the Keith Ligon lab. Cells were routinely fingerprinted for identity validation and tested (at least every 3 months) for mycoplasma infection using the MycoAlert Mycoplasma Detection Kit (Lonza, LT07-318), according to the manufacturer's instructions.

Culturing of hNSCs

hNSCs were maintained on adherent plates pretreated with Geltrex LDEV-Free Reduced Growth Factor Basement Membrane Matrix (Gibco, A1413201) for at least 30 minutes. hNSCs were grown in

culture medium containing a 1:1 ratio of DMEM/F-12 (Invitrogen, 11330-032) and Neurobasal A (Invitrogen, 10888-022) with 1% each of HEPES Buffer Solution 1M (Thermo Fisher, 15630080), Sodium Pyruvate Solution 100 nM (Life Technologies, 11360070), MEM Non-Essential Amino Acids Solution 10 mM (Thermo Fisher, 11140050), Glutamax-I Supplement (Thermo Fisher, 35050061) and Penicillin/Streptomycin Solution (Life Technologies, 15140122). Media was supplemented with B-27 minus vitamin A (Invitrogen, 12587-010), epidermal growth factor (StemCell Tech. Inc., 78006), fibroblast growth factor (GF003, StemCell Tech. Inc., 78003) and 0.2% heparin solution (StemCell Tech. Inc., 07980). Culture media was replaced with fresh media every 48 hours and cells were dissociated using Accutase (StemCell Tech. Inc., 07922) to be passaged every 4 days.

Culturing of Lenti-X HEK293T cells

Lenti-X HEK293T were maintained on adherent plates and grown in culture medium of DMEM (Thermo Fisher, 11965092) supplemented with 10% of BenchMark Fetal Bovine Serum (GeminiBio, 100-106). Cells were dissociated using Trypsin-EDTA (0.25%) (Thermo Fisher, 25200114) to be passaged every 3 to 4 days.

Culturing of patient-derived DMG lines

BT245 and SF7761 cell lines were grown in tumor stem media containing a 1:1 ratio of DMEM/F-12 (Invitrogen, 11330-032) and Neurobasal-A (Invitrogen, 10888-022) with 10% each of HEPES Buffer Solution 1 M (Thermo Fisher, 15630080), sodium pyruvate solution 100 nmol/L (Life Technologies, 11360070), MEM nonessential amino acids solution 10 mmol/L (Thermo Fisher, 11140050), Glutamax-I Supplement (Thermo Fisher, 35050061), and penicillin/streptomycin solution (Life Technologies, 15140122). Media was supplemented with B27 minus Vitamin A (Invitrogen, 12587-010), EGF, StemCell Tech Inc., 78006), FGF, StemCell Tech Inc., 78003), and heparin solution 0.2% (StemCell Tech Inc., 07980). Cells were dissociated using Accutase (StemCell Tech. Inc., 07922) to be passaged every 4 days.

Culturing of OPCs

OPC cell line and optimized culture media kit was purchased from EMD Millipore Sigma and passaged according to manufacturer's instructions. Cells were grown on Matrigel-coated adherent plates. Cells were dissociated using Accutase (StemCell Tech. Inc., 07922) to be passaged every 7-10 days.

Lentiviral production and transductions

Plasmid generation

Primers were designed and ordered from Integrated DNA Technologies (Newark, NJ) for PCR amplification of desired inserts of H3F3A wild-type (WT) and H3F3A K27M with or without N or C terminal tags. PCR amplification was performed using full-length WT or K27M variations of the gene with N-terminal FLAG+HA tag as templates with the following cycle: 94°C for 2 min, followed by 30 cycles of 94°C for 10 min, 55 °C for 10 min, and 70°C for 15 min, with a final extension of 2 min at 70 °C. Insert DNA fragments were then purified using the QIAquick PCR Purification Kit (Qiagen, 28104) according to manufacturer's instructions. Closed pLX312 vector obtained from the Broad Genetics Perturbation Platform (GPP) and insert DNA fragments were digested in a reaction mix consisting of 2 µL ClaI (New England BioLabs, R0197S), 1 µL EcoRV-HF (New England BioLabs, R3195S), 5 µL 1X NEBuffer (New England BioLabs, B6002S), 1 µg DNA, and ddH2O up to a total reaction mixture of 50 µL. Digestion proceeded for 2 hours at room temperature. Digested insert DNA fragments were then purified using the QIAquick PCR Purification Kit (Qiagen, 28104) and digested vector was gel extracted using the QIAquick Gel Extraction Kit (Qiagen, 28704) according to manufacturer's instructions. Digested insert DNA fragments were ligated to the open vector at a 3:1 molar ratio using 2 µL 10X Ligase Buffer (New England Biolabs, B0202S), 1 µL T4 Ligase (New England Biolabs, M0202L), and ddH2O up to a total reaction mixture of 20 µL. Ligation proceeded at room temperature for 2 hours and was heat-inactivated at 65°C for 10 minutes. Then, 10 µL of the ligation reaction was added to 50 µL of One Shot Stbl3 Chemically Competent E. coli (Invitrogen, C737303) and placed on ice for 30 minutes.

The cells were then heat shocked at 42°C for 30 seconds and incubated on ice for 5 minutes. SOC media (Invitrogen, 15544034) was subsequently added to cells to allow for recovery and then shaken for 1 hour at 37°C. Transformants were plated on LB agar plates containing 100 µg/mL of carbenicillin and grown at 37°C for no more than 18 hours. Minipreps were performed using the QIAprep Spin Miniprep Kit (Qiagen, 27104) and sequences were verified by Plasmidsaurus whole plasmid sequencing. Once sequences were verified, Maxipreps were performed using the ZymoPURE II Plasmid Maxiprep Kit (Zymo Research, D4202).

Virus production

Lenti-X 293T cells (Takara Bio, 632180) were transfected with 10 µg of lentiviral expression vectors with packaging plasmids encoding PSPAX2 and VSVG using Lipofectamine 3000 (Thermo Fisher, L3000075). Media was replaced 6 hours after transfection. Supernatant containing lentivirus was collected 24 hours later, concentrated using the Lenti X-Concentrator (Takara, 631231) according to the manufacturer's instructions, and collected in DMEM (Thermo Fisher, 11965092).

Transductions

hNPCs and Lenti-X 293T cells were seeded at 1.3 x 10^5 cells/mL in adherent 10 cm dishes (CELLTREAT, 229620) and infected using no-spin infection 24 hours later. Dishes for hNPCs were pretreated with Geltrex LDEV-Free Reduced Growth Factor Basement Membrane Matrix (Gibco, A1413201) for at least 30 minutes. Infected cells were subsequently flow-sorted for GFP-positive cells 24 hours after infection.

Fluorescence-activated cell sorting

Cells were passaged as per routine cell culture methods and gated based on GFP expression with non-GFP-expressing cells used as negative controls. Cells were subsequently flow sorted on a BD FACSAria III directly into 15 cm tubes containing appropriate media.

Histone extraction and immunoblotting

Two-step histone extraction was performed on cells using the Histone Extraction Kit (Active Motif, 40028) according to manufacturer's instructions. Supernatant was quantified with the Pierce 660 nm Protein Assay (Thermo Fisher, 22660), mixed with NuPAGE LDS Sample Buffer 4X (Invitrogen, NP0008), and heated at 90°C for 5 min. Equal amounts of protein for each sample were loaded alongside Cytiva Rainbow Molecular Weight Marker (Thermo Fisher, 45-001-591) and separated by SDS-PAGE on NuPAGE™ Bis-Tris Mini Protein Gels, 4–12% (Invitrogen, NP0321). Blots were subsequently dry transferred using the iBlot 2 Gel Transfer Device (Thermo Fisher, IB21001), placed in AdvanBlock-Chemi blocking solution (Advansta, R-03726-E10), and gently agitated for 1 hour at room temperature. Blots were then put in primary antibody and gently agitated at 4 °C overnight before being washed with 1X TBST three times for 15 minutes each. Antibodies against the following proteins were used with indicated dilutions in this study: Histone H3-HRP (Cell Signaling, 12648), Tri-Methyl-Histone H3 (Lys27) (Cell Signaling, 9733), HA-Tag (Cell Signaling, 3724), V5-Tag (Cell Signaling, 13202), and DYKDDDDK Tag (Cell Signaling, 2368). Blots were then put in secondary antibody (Anti-rabbit IgG, HRP-linked antibody, Cell Signaling, 7074) (1:10,000) and gently agitated for one hour at room temperature before being washed with 1X TBST three times for 15 minutes each. Blots were saturated in SuperSignal West Femto Maximum Sensitivity Substrate (Thermo Fisher, 34095) and visualized on the Fujifilm LAS-3000 Imaging System.

Immunoblot quantification

Quantification of the relative band intensities in the Western immunoblots was performed using the ImageJ/Fiji v2.14.0 software. Images with no overexposed pixels were selected for analysis. To measure band intensity, the Fiji Gel Analyzer tool was used to integrate pixel values across the length of the band. Background subtraction was performed on a per-lane basis to account for possible differences in exposure across the blot. To compare H3K27me3 intensity across samples, the ratio of

H3K27me3 integrated intensity was normalized to H3-Total loading intensity. For samples with N≥3 replicates, statistical testing was performed with two-sided t-testing, assuming equal variance across samples, using Graphpad Prism to compare the H3K27me3:H3-Total ratio of the given sample against the H3K27me3:H3-Total ratio of the respective untransduced control line. Graphs of H3K27me3 levels were generated by normalizing the sample H3K27me3:H3-Total ratio against H3K27me3-H3Total ratio of the untransduced control line.

Integrated DNA Technologies oligos

H3.3-Tagless-Forward

GGTGGTATCGATATGGCTCGTACAAAGCAGACTGCC

H3.3-Tagless-Reverse

GGTGGTGATATCTCAAGCACGTTCTCCACGTATGCG

H3.3-Nterm-FLAG-Forward

GGTGGTATCGATATGTACAAGGACGACGATGACAAGGCTCGTACAAAGCAGACTGCC

H3.3-Nterm-HA-Forward

GGTGGTATCGATATGTACCCATACGATGTTCCAGATTACGCTGCTCGTACAAAGCAGACTGCC

H3.3-Nterm-V5-Forward

GGTGGTATCGATATGGGTAAGCCTATCCCTAACCCTCTCCTCGGTCTCGATTCTACGGCTCGTACAAAGCAGACTGCC

H3.3-Nterm-HAorFLAGorV5-Reverse

GGTGGTGATATCTCAAGCACGTTCTCCACGTATGCG

H3.3-Cterm-HAorFLAGorV5-Forward

GGTGGTATCGATATGGCTCGTACAAAGCAGACTGCC

H3.3-Cterm-FLAG+HA-Reverse

GGTGGTGATATCCTAAGCGTAATCTGGAACATCGTATGGGTACTTGTCATCGTCGTCCTTGTAAGCACGTTCTCCACGTATGCG

References

1. Jenuwein, T. & Allis, C. D. Translating the Histone Code. *Science* **293**, 1074–1080 (2001).

2. Khuong-Quang, D.-A. *et al.* K27M mutation in histone H3.3 defines clinically and biologically distinct subgroups of pediatric diffuse intrinsic pontine gliomas. *Acta Neuropathol. (Berl.)* **124**, 439–447 (2012).

3. Schwartzentruber, J. *et al.* Driver mutations in histone H3.3 and chromatin remodelling genes in paediatric glioblastoma. *Nature* **482**, 226–231 (2012).

4. Lewis, P. W. *et al.* Inhibition of PRC2 Activity by a Gain-of-Function H3 Mutation Found in Pediatric Glioblastoma. *Science* **340**, 857–861 (2013).

5. Harutyunyan, A. S. *et al.* H3K27M induces defective chromatin spread of PRC2-mediated repressive H3K27me2/me3 and is essential for glioma tumorigenesis. *Nat. Commun.* **10**, 1262 (2019).

6. Harutyunyan, A. S. *et al.* H3K27M in Gliomas Causes a One-Step Decrease in H3K27 Methylation and Reduced Spreading within the Constraints of H3K36 Methylation. *Cell Rep.* **33**, (2020).

7. Stafford, J. M. *et al.* Multiple modes of PRC2 inhibition elicit global chromatin alterations in H3K27M pediatric glioma. *Sci. Adv.* **4**, eaau5935 (2018).

8. Tagami, H., Ray-Gallet, D., Almouzni, G. & Nakatani, Y. Histone H3.1 and H3.3 Complexes Mediate Nucleosome Assembly Pathways Dependent or Independent of DNA Synthesis. *Cell* **116**, 51–61 (2004).

9. Kaludov, N. K., Pabón-Peña, L., Seavy, M., Robinson, G. & Hurt, M. M. A Mouse Histone H1 Variant, H1b, Binds Preferentially to a Regulatory Sequence within a Mouse H3.2 Replication-dependent Histone Gene *. *J. Biol. Chem.* **272**, 15120–15127 (1997).

10. Wu, R. S., Tsai, S. & Bonner, W. M. Patterns of histone variant synthesis can distinguish go from G1 cells. *Cell* **31**, 367–374 (1982).

11. Goldberg, A. D. *et al.* Distinct factors control histone variant H3.3 localization at specific genomic regions. *Cell* **140**, 678–691 (2010).

12. Funato, K., Major, T., Lewis, P. W., Allis, C. D. & Tabar, V. Use of human embryonic stem cells to model pediatric gliomas with H3.3K27M histone mutation. *Science* **346**, 1529–1533 (2014).

13. Haag, D. *et al.* H3.3-K27M drives neural stem cell-specific gliomagenesis in a human iPSC-derived model. *Cancer Cell* **39**, 407-422.e13 (2021).

14. Brien, G. L. *et al.* Simultaneous disruption of PRC2 and enhancer function underlies histone H3.3-K27M oncogenic activity in human hindbrain neural stem cells. *Nat. Genet.* **53**, 1221–1232 (2021).

15. Jessa, S. *et al.* K27M in canonical and noncanonical H3 variants occurs in distinct oligodendroglial cell lineages in brain midline gliomas. *Nat. Genet.* **54**, 1865–1880 (2022).

Conflict of Interest

PB and RB have received grant funding from Novartis Institute of Biomedical Research for an unrelated project. PB has served on paid Advisory Boards for QED Therapeutics, and DayOne Biopharmaceuticals. RB owns equity in and consults for Scorpion Therapeutics. All remaining authors declare no competing interests.

Contributions

NP, RB, and PB conceived and designed the experiments, interpreted results, and wrote the manuscript. DFZ and AFK assisted with experimental design, execution and interpretation. IG and OEF assisted with experimental execution.
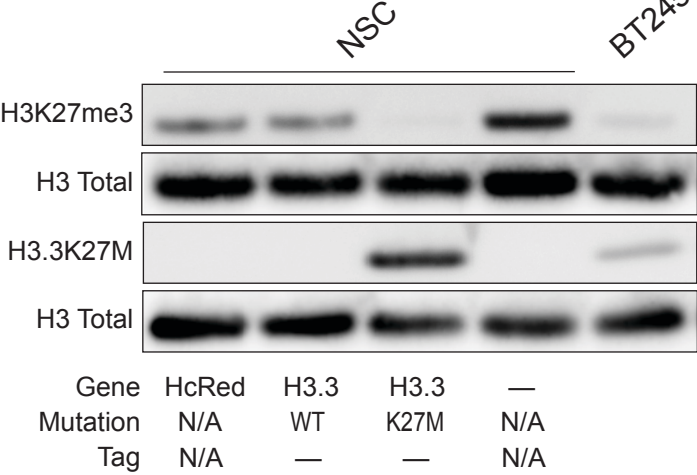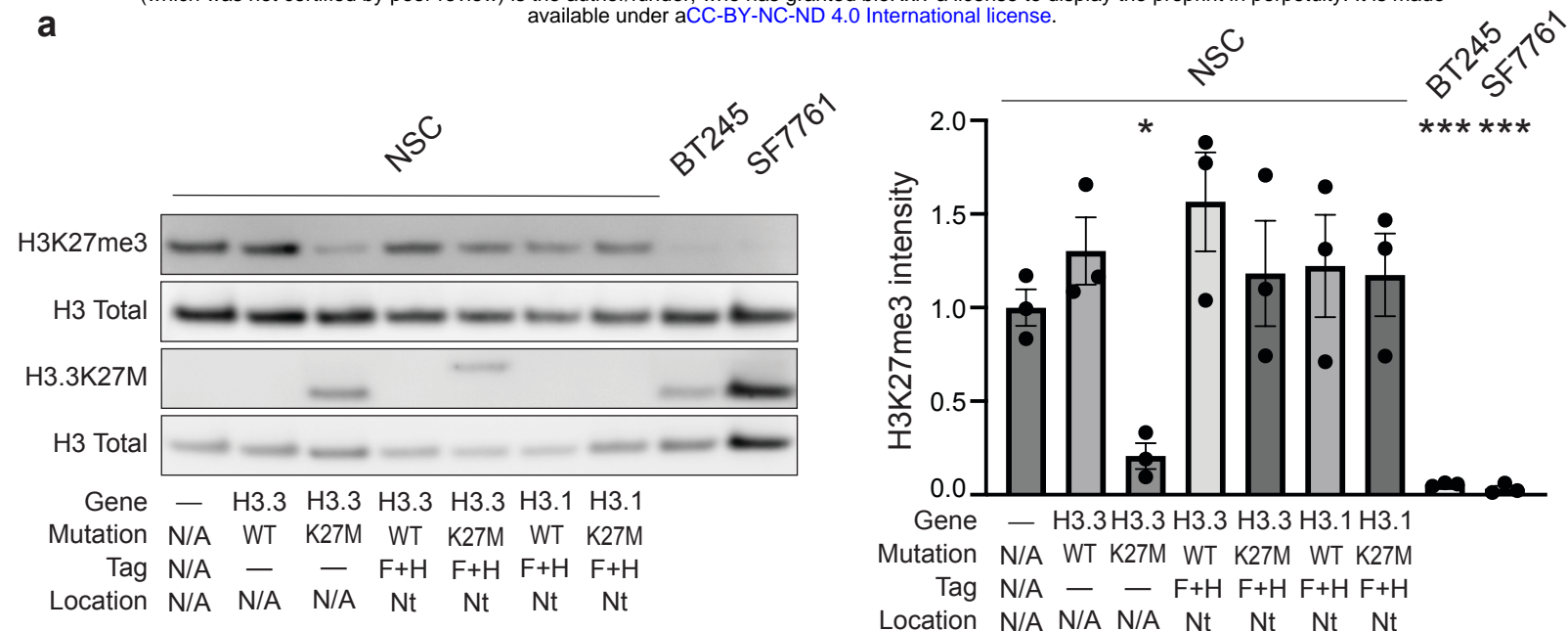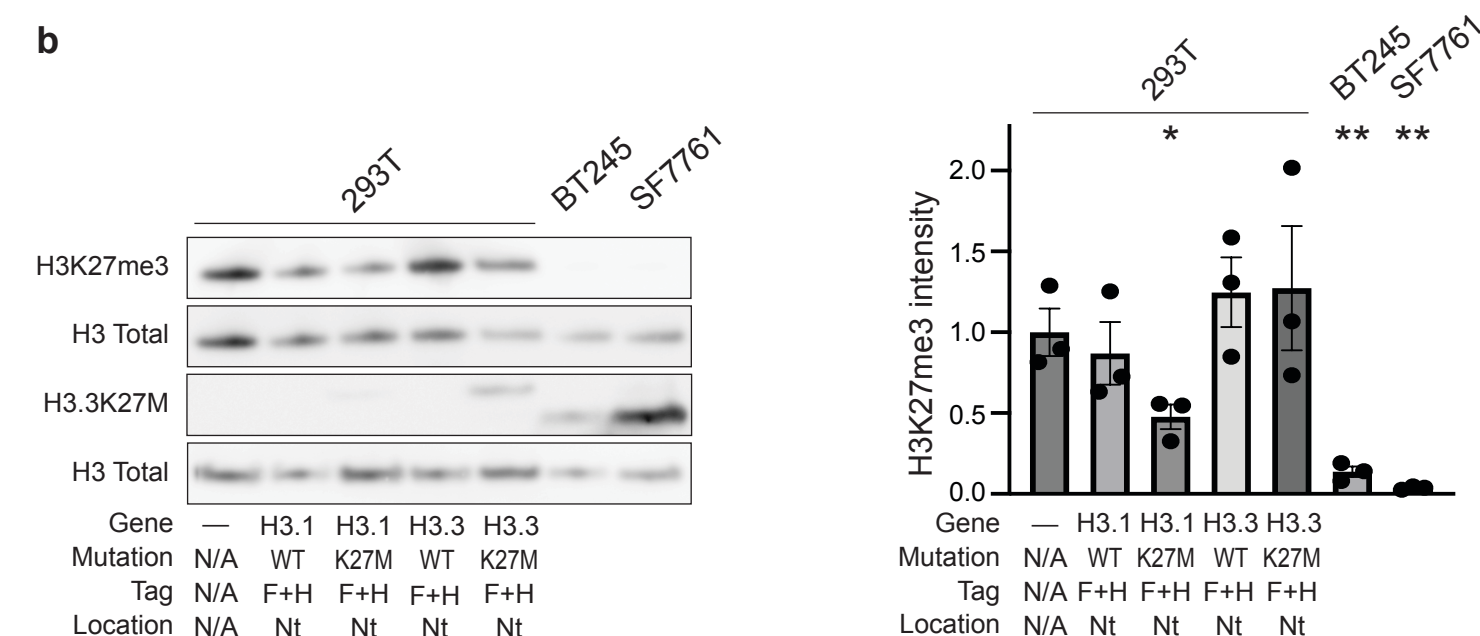
Figure 1

Figure 1. Overexpression of untagged H3.3K27M in NSCs drives reduction of H3K27me3 levels

Western immunoblot comparing H3K27me3 levels in NSCs overexpressing the HcRed, H3.3WT, or H3.3K27M transgenes, or untransduced control. Lysates from the BT245 patient-derived DMG cell line are included as a control for H3K27me3 loss.
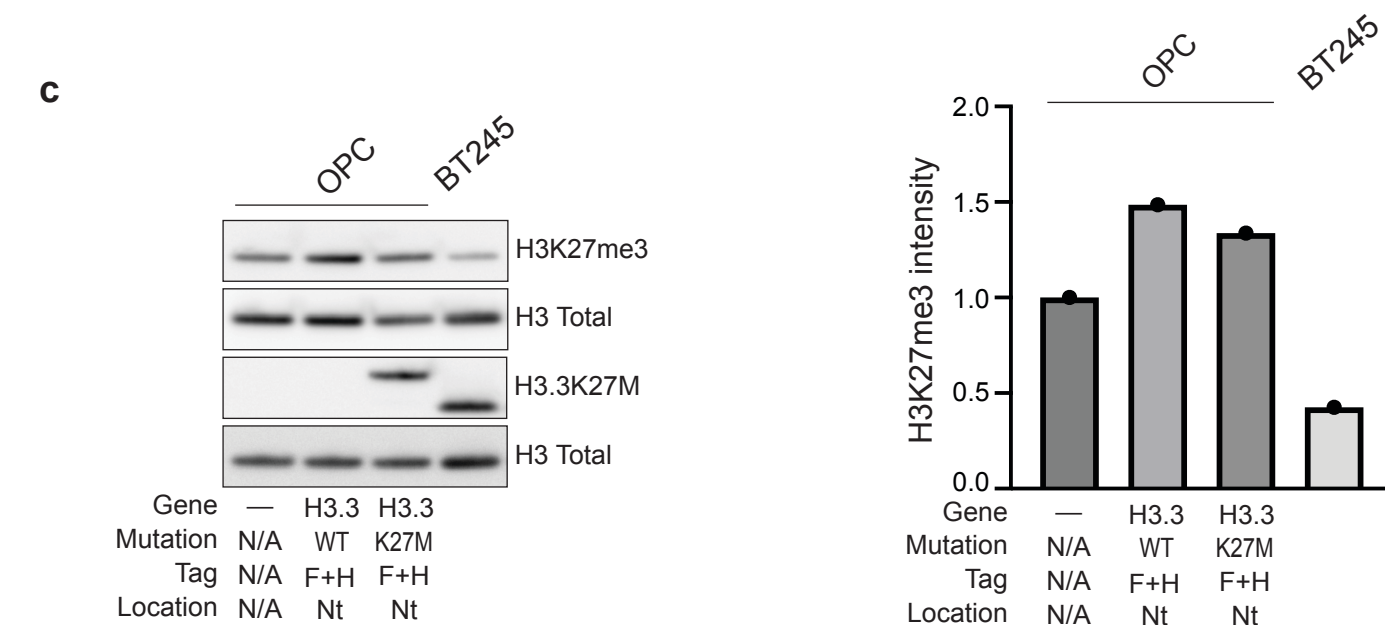
Figure 2. N-terminal FLAG+HA tag inhibits H3K27M-mediated reduction in H3K27me3 levels
a. Left: Western immunoblot of NSCs overexpressing N-terminal (Nt) tagged H3.3 or H3.1, and their respective K27M mutants, compared to untagged H3.3 controls, or the patient-derived DMG lines BT245 and SF7761. Right: quantification of H3K27me3 levels, normalized to H3-total loading and plotted as a fraction of the signal from the untransduced NSC control. Error bars, mean $\pm$ SEM of three replicates per condition. Significance testing performed with t-test against untransduced NSC sample. **b.** Left: Western immunoblot of HEK293T cells overexpressing N-terminal tagged H3.1 or H3.3 (and their respective K27M mutants), compared to the patient-derived DMG lines BT245 and SF7761. Right: quantification of H3K27me3 levels, normalized to H3-total loading and plotted as a fraction of the signal from the untransduced HEK293T. Error bars, mean $\pm$ SEM of three replicates per condition. Significance testing performed with t-test against untransduced HEK293T control. **c.** Left: Western immunoblot of OPCs overexpressing N-terminal tagged H3.3WT or H3.3K27M mutants compared to the BT245 patient-derived DMG line. Right: quantification of H3K27me3 levels, normalized to H3-total loading and plotted as a fraction of the signal from the untransduced OPC control. One replicate per condition. * = p<0.05, **=p<0.01, ***=p<0.001.
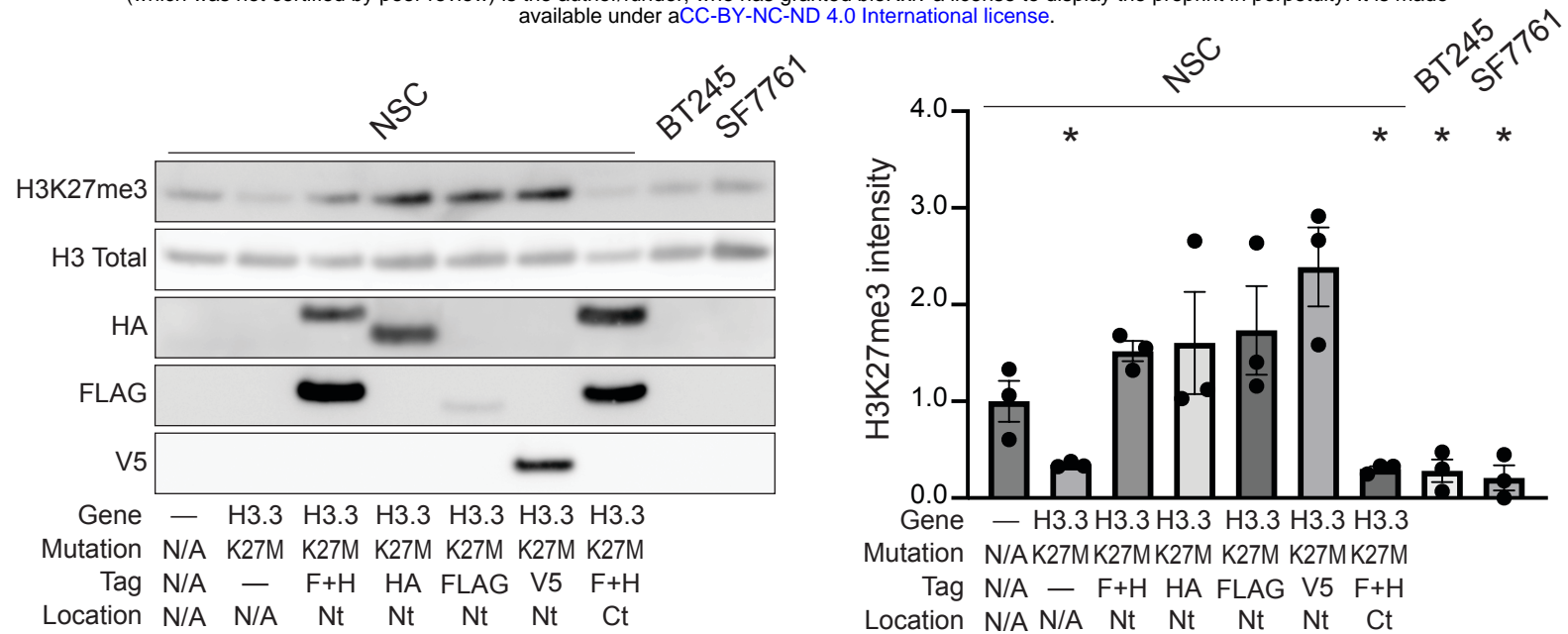
Figure 3

Figure 3. Multiple N-terminal tags inhibit H3K27M-mediated reduction in H3K27me3 levels

Left: Western immunoblot comparing H3K27me3 levels in NSCs overexpressing H3.3K27M with the indicated N-terminal (Nt) or C-terminal (Ct) tag compared to the patient-derived DMG lines BT245 and SF7761. Right: quantification of H3K27me3 levels, normalized to H3-total loading and plotted as a fraction of the signal from the untransduced NSC control. Error bars, mean $\pm$ SEM of three replicates per condition. Significance testing performed with t-test against untransduced NSC sample, * = p<0.05, **=p<0.01, ***=p<0.001